SOCIETÀ TOSCANA
DI
SCIENZE NATURALI
RESIDENTE IN PISA

ATTI
DELLA
SOCIETÀ TOSCANA
DI
SCIENZE NATURALI

MEMORIE • SERIE A • VOLUME CXXV • ANNO 2018

Edizioni ETS

UNIVERSITÀ DI PISA
MUSEO DI STORIA NATURALE

Con il contributo del Museo di Storia Naturale dell’Università di Pisa

Fondazione
Cassa di Risparmio
di Lucca

e della Fondazione Cassa di Risparmio di Lucca

INDICE - *CONTENTS*

D. Mauro, C. Biagioni, M. Pasero, F. Zaccarini, *Crystal-chemistry of sulfates from Apuan Alps (Tuscany, Italy). II. Crystal structure and hydrogen bonding system of römerite,* $Fe^{2+}Fe^{3+}_2(SO_4)_4(H_2O)_{14}$.
Cristallochimica dei solfati delle Alpi Apuane (Toscana, Italia). II. Struttura e legami a idrogeno della römerite, $Fe^{2+}Fe^{3+}_2(SO_4)_4(H_2O)_{14}$. pag. 5

E.J. Anthony, *Sand and gravel supply from rivers to coasts: A review from a Mediterranean perspective.*
L'apporto di sabbia e ghiaia dai fiumi alle coste: una review dal punto di vista del Mediterraneo. » 13

L. Jaselli, A. Collareta, *Redescription and first illustration of the holotype of* Astropecten montalionis *(Meneghini, 1852) [Paxillosida: Astropectinidae].*
Ridescrizione e prima illustrazione dell'olotipo di *Astropecten montalionis* (Meneghini, 1852) [Paxillosida: Astropectinidae]. » 35

F. Rapetti, *L'alluvione di Livorno del 10 settembre 2017 (Toscana, Italia).*
Leghorn flood on September 10 2017 (Tuscany, Italy). » 45

D. Bertoni, M. Mencaroni, *Four different coastal settings within the Northern Tuscany littoral cell: how did we get here?*
Quattro diversi ambienti costieri all'interno della cella litoranea della Toscana settentrionale: come siamo arrivati a questo punto? » 55

D. Pieruccioni, S. Vezzoni, M. Petrelli, *A petrographic and U-Pb geochronological approach to the reconstruction of the pre-Alpine history of Alpi Apuane (Tuscany).*
Un approccio petrografico e geocronologico U-Pb per la ricostruzione della storia pre-Alpina delle Alpi Apuane (Toscana). » 69

A. Gatti, P. Marianelli, D. Andronico, A. Sbrana, *The December 2015 paroxysms at Mt. Etna: insights from mineral chemistry and glasses.*
L'eruzione parossistica dell'Etna del dicembre 2015: indicazioni sul comportamento del sistema di alimentazione dallo studio di minerali e vetri. » 81

P. R. Federici, S. Merlino, R. Grifoni, *In memoria di Aldo Giacomo Segre (1918-2018).*
In Memoriam Aldo Giacomo Segre (1918-2018). » 93

Processi Verbali - http://www.stsn.it. » 101

Atti Soc. Tosc. Sci. Nat., Mem., Serie A, 125 (2018)
pagg. 5-11, fig. 4; tab. 6; *doi: 10.2424/ASTSN.M.2018.19*

Daniela Mauro (1), Cristian Biagioni (1), Marco Pasero (1), Federica Zaccarini (2)

CRYSTAL-CHEMISTRY OF SULFATES FROM APUAN ALPS (TUSCANY, ITALY). II. CRYSTAL STRUCTURE AND HYDROGEN BONDING SYSTEM OF RÖMERITE, $Fe^{2+}Fe^{3+}_2(SO_4)_4(H_2O)_{14}$

Abstract - D. Mauro, C. Biagioni, M. Pasero, F. Zaccarini, *Crystal-chemistry of sulfates from Apuan Alps (Tuscany, Italy). II. Crystal structure and hydrogen bonding system of römerite,* $Fe^{2+}Fe^{3+}_2(SO_4)_4(H_2O)_{14}$.
Römerite, ideally $Fe^{2+}Fe^{3+}_2(SO_4)_4(H_2O)_{14}$, from the Fornovolasco mine (Apuan Alps, Tuscany, Italy) has been characterized through electron microprobe analysis, micro-Raman spectroscopy, and X-ray diffraction. Römerite occurs as pinkish microcrystalline aggregates or as rare euhedral brownish crystals, up to some mm in size. Electron microprobe analysis (in wt% - average of ten spot analyses) gave: SO_3 40.46(94), FeO_{tot} 26.64(94), MgO 1.14(11), total 68.25(104). Assuming the occurrence of 14 H_2O groups per formula unit and recalculating the Fe^{2+}:Fe^{3+} atomic ratio according to the structure refinement, the chemical formula can be written as $(Fe^{2+}_{0.82}Mg_{0.22})_{\Sigma 1.04}Fe^{3+}_{2.08}S_{3.95}O_{16}\cdot 14H_2O$. The Raman spectrum of römerite is characterized by the four fundamental modes of SO_4 groups and by bending and stretching vibrations of H_2O groups. Raman bands at wavenumbers lower than 400 cm^{-1} are related to Fe-O vibrational modes. Römerite crystallizes in the space group $P\bar{1}$, with unit-cell parameters $a = 6.4512(6)$, $b = 15.323(2)$, $c = 6.3253(6)$ Å, $\alpha = 90.131(5)$, $\beta = 100.900(4)$, $\gamma = 85.966(4)°$, $V = 612.41(10)$ Å^3, $Z = 1$. The crystal structure of römerite has been refined to $R_1 = 0.023$ on the basis of 4346 reflections with $F_o > 4\sigma(F_o)$ and 226 refined parameters. The crystal structure of römerite is formed by isolated $\{Fe^{2+}(H_2O)_6\}$ octahedra and $[Fe^{3+}(SO_4)_2(H_2O)_4]$ clusters, bonded through H-bonds.

Key words - römerite, sulfate mineralogy, crystal structure, hydrogen bonds, Fornovolasco, Apuan Alps.

Riassunto - D. Mauro, C. Biagioni, M. Pasero, F. Zaccarini, *Cristallochimica dei solfati delle Alpi Apuane (Toscana, Italia). II. Struttura e legami a idrogeno della römerite,* $Fe^{2+}Fe^{3+}_2(SO_4)_4(H_2O)_{14}$.
La römerite, idealmente $Fe^{2+}Fe^{3+}_2(SO_4)_4(H_2O)_{14}$, della miniera di Fornovolasco (Alpi Apuane, Toscana, Italia) è stata caratterizzata tramite analisi in microsonda elettronica, spettroscopia micro-Raman e diffrazione di raggi X. Questo minerale compare sotto forma di aggregati microcristallini rosati o rari cristalli euedrali brunastri, grandi fino ad alcuni mm. L'analisi chimica in microsonda ha fornito i seguenti risultati (in wt% - media di 10 analisi puntuali): SO_3 40.46(94), FeO_{tot} 26.64(94), MgO 1.14(11), totale 68.25(104). Assumendo la presenza di 14 gruppi H_2O per unità formula e ricalcolando il rapporto atomico Fe^{2+}:Fe^{3+} in accordo con i dati strutturali, la formula chimica della römerite può essere scritta $(Fe^{2+}_{0.82}Mg_{0.22})_{\Sigma 1.04}Fe^{3+}_{2.08}S_{3.95}O_{16}\cdot 14H_2O$. Lo spettro Raman è caratterizzato dai quattro modi vibrazionali fondamentali dei gruppi SO_4 e dalle vibrazioni di *bending* e di *stretching* dei gruppi H_2O. Le bande Raman con frequenze inferiori a 400 cm^{-1} sono legate a modi vibrazionali dei legami Fe-O. La römerite cristallizza nel sistema triclino, gruppo spaziale $P1$, con parametri di cella $a = 6.4512(6)$, $b = 15.323(2)$, $c = 6.3253(6)$ Å, $\alpha = 90.131(5)$, $\beta = 100.900(4)$, $\gamma = 85.966(4)°$, $V = 612.41(10)$ Å^3, $Z = 1$. La sua struttura è stata raffinata fino ad un fattore di accordo $R_1 = 0.023$ sulla base di 4346 riflessi con $F_o > 4\sigma(F_o)$ and 226 parametri raffinati. La struttura della römerite è costituita da ottaedri isolati $\{Fe^{2+}(H_2O)_6\}$ e gruppi $[Fe^{3+}(SO_4)_2(H_2O)_4]$, uniti fra loro tramite legami a H.

Parole chiave - römerite, solfati, struttura, legami a idrogeno, Fornovolasco, Alpi Apuane.

INTRODUCTION

Römerite is a hydrated iron sulfate having ideal formula $Fe^{2+}Fe^{3+}_2(SO_4)_4\cdot 14H_2O$, commonly occurring as an oxidation product of sulfides in coal and ore deposits, whereas it is rarer in volcanic environments (Jambor *et al*., 2000). In some localities, it may be sufficiently abundant to be exploited as a sulfuric acid source, such as at the Alcaparrosa deposit, Chile (Bandy, 1938). Together with lishizenite, $Zn^{2+}Fe^{3+}_2(SO_4)_4\cdot 14H_2O$ (Lin & Chen, 1990), it forms the römerite group. Likely, the unnamed mineral "UM1968-03-SO:FeHMg" (Smith & Nickel, 2007), reported by Oleinikov & Shvartsev (1968), could be the magnesium analogue of römerite. Römerite was first found by Grailich (1858) in the Rammelsberg mine, Harz, Lower Saxony, Germany. Its cell setting was first investigated through X-ray diffraction by Van Loan & Nuffield (1959), whose results agreed with the cell setting proposed by Wolfe (1937) on the basis of morphological studies. The crystal structure of römerite was solved by Fanfani *et al.* (1970) on the basis of film data using a sample from the Dexter mine, Utah, USA. The refinement, converging at $R = 0.061$, allowed the location of the H positions. In the framework of the study of sulfate assemblages from Tl-rich pyrite ores of southern Apuan Alps (Tuscany, Italy) (*e.g.*, Mauro *et al*., 2018), well-crystallized specimens of römerite, suitable for single-crystal X-ray diffraction, were collected. The aim of this paper is to describe this occurrence and to improve the knowledge of the structural arrangement of this mineral through the description of the results obtained using high-quality data collected through a CCD device.

---

(1) Dipartimento di Scienze della Terra, Università di Pisa, Via Santa Maria 53, I-56126 Pisa. *Corresponding author e-mail*: cristian.biagioni@unipi.it
(2) Department of Applied Geological Sciences and Geophysics, University of Leoben, Peter Tunner Str. 5, A-8700 Leoben.

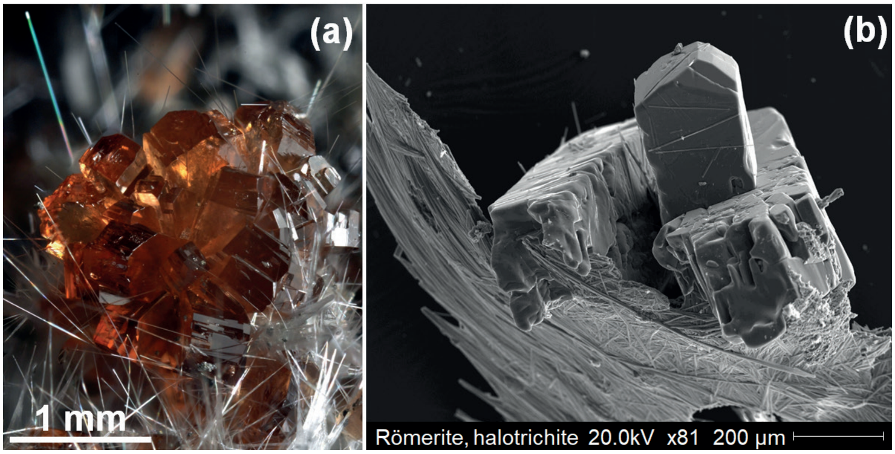

Fig. 1 - Römerite from Fornovolasco (Apuan Alps, Tuscany, Italy), as aggregates of brown-orange triclinic crystals associated with white acicular individuals of halotrichite (a); the morphology of römerite crystals, with well-developed {010} and {001} forms, can be observed through SEM (b).

EXPERIMENTAL

The studied specimen of römerite was collected in the pyrite – iron oxide mine of Fornovolasco (Fabbriche di Vergemoli, Apuan Alps, Tuscany, Italy). Römerite is one of the main minerals in the sulfate pile occurring in the old tunnels of the 740 m level of the Fornovolasco mine and described by Biagioni *et al.* (2011). It occurs as microcrystalline pinkish masses or, rarely, as euhedral crystals, up to 1 mm in size (Fig. 1). Römerite is typically associated with halotrichite, copiapite, melanterite, and, more rarely, with voltaite, alum-(K), alunogen, and coquimbite.

Chemical data

Preliminary qualitative chemical analyses were performed using a Philips XL 30 scanning electron microscope equipped with an EDAX DX-4 system operating in energy-dispersive mode. Iron, S and minor Mg were found as the only elements with $Z > 8$ above the detection limit. Quantitative chemical data were collected through a Superprobe JEOL JXA 8200 electron microprobe at the "Eugen F. Stumpfl" laboratory, Leoben University, Austria, using the following analytical conditions: WDS mode, accelerating voltage 10 kV and beam current 10 nA. The beam size was set to 20 μm in order to avoid sample damage. The following standards (element, emission line) were used: magnetite (Fe$K\alpha$), olivine (Mg$K\alpha$), and NiS (S$K\alpha$). The ZAF routine was applied for the correction of recorded raw data. Counting times were 15 s for peak and 5 s for backgrounds. The following results were obtained (in wt% - average of ten spot analyses): SO_3 40.46(94), FeO_{tot} 26.64(94), MgO 1.14(11), total 68.25(104). Assuming the occurrence of 14 H_2O groups per formula unit and recalculating the Fe^{2+}:Fe^{3+} atomic ratio according to the structure refinement, the chemical composition of the studied sample is (in wt%) SO_3 40.46, Fe_2O_3 21.24, FeO 7.56, MgO 1.14, H_2O 32.28, total 102.65, corresponding, on the basis of 30 O atoms per formula unit, to the chemical formula $(Fe^{2+}_{0.82}Mg_{0.22})_{\Sigma 1.04}Fe^{3+}_{2.08}S_{3.95}O_{16}\cdot 14H_2O$. The slightly higher than ideal total is likely related to the partial dehydration of römerite under the electron beam. The occurrence of minor Mg replacing Fe^{2+} is in keeping with the occurrence of the Mg analogue of römerite reported by Oleinikov & Shvartsev (1968).

Micro-Raman spectroscopy

Unpolarized micro-Raman spectra were collected on unpolished samples of römerite in nearly backscattered geometry with a Jobin-Yvon Horiba XploRA Plus apparatus, equipped with a motorized *x-y* stage and an Olympus BX41 microscope with a 10× objective lens. The Raman spectra were excited using a 532 nm line of a solid-state laser attenuated to 10% in order to minimize sample damage. The minimum lateral and depth resolution was set to a few μm. The system was calibrated using the 520.6 cm^{-1} Raman band of silicon before each experimental session. Spectra were collected through multiple acquisitions with single counting times of 60 s. Backscattered radiation was analyzed with a 1200 mm^{-1} grating monochromator.

The Raman spectrum of römerite is shown in Figure 2. The position of the observed Raman bands and their interpretation are given in Table 1. In the region between 400 and 1300 cm^{-1}, the Raman spectrum of römerite is characterized by bending and stretching modes of the SO_4 groups. The occurrence of multiple bands for the SO_4 groups agrees with the presence of two structurally different SO_4 units, as suggested by previous authors (*e.g.*, Chio *et al.*, 2005; Frost *et al.*, 2011) and confirmed by the structural investigation. Lattice and Fe-O modes occur in the range 100-300 cm^{-1}.

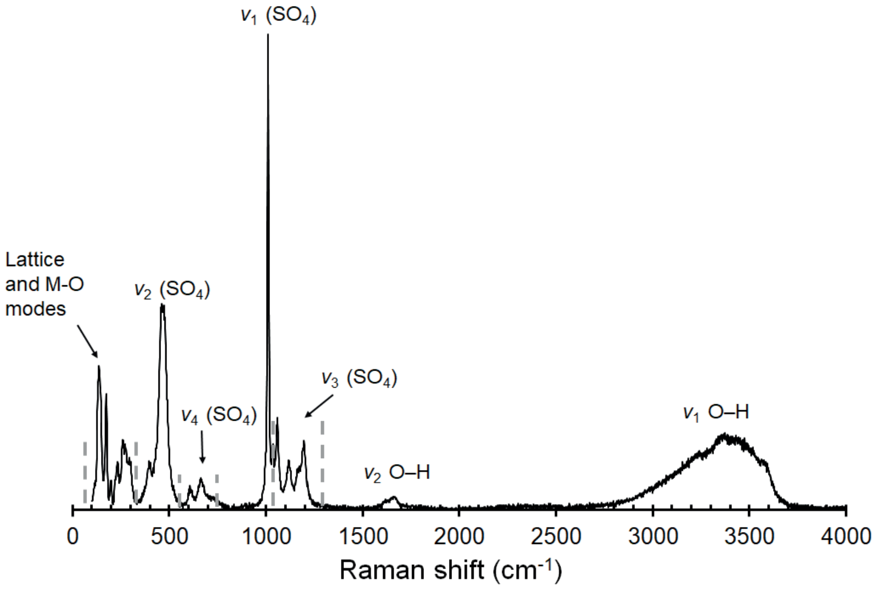

Fig. 2 - Raman spectrum of römerite. The interpretation of the bands is shown.

Table 1 - Raman bands (in cm^{-1}) and interpretation of the micro-Raman spectrum of römerite.

	SO_4 vibration modes		
ν_1	ν_2	ν_3	ν_4
1011	400	1059	607
1035	463	1118	664
		1167	
		1197	
	H_2O vibration modes		
	ν_1	ν_2	
	3234	1654	
	3357		
	3460		
	3570		
	M-O and lattice modes		
	147	261	
	177	264	
	200	274	
	232	293	

The occurrence of H_2O groups is confirmed by the presence of bending and stretching modes of O-H bonds. The former is represented by a weak band at 1654 cm^{-1}, whereas the latter gives rise to a broad band between 3000 and 3600 cm^{-1}. The occurrence of several bands suggests the presence of several non-equivalent H-bonds in the crystal structure of römerite.

X-ray crystallography

Intensity data were collected using a Bruker Smart Breeze diffractometer operating at 50 kV and 30 mA and equipped with an air-cooled CCD detector. Graphite-monochromatized Mo*K*α radiation was used. The detector-to-crystal working distance was set to 50 mm. A total of 2505 frames were collected using φ and ω scan modes, with an exposure time of 5 seconds per frame. Intensity data were integrated and corrected for Lorentz, polarization, background effects, and absorption using the package of software *Apex* 2 (Bruker AXS Inc., 2004). The statistical tests on the distribution of $|E|$ values ($|E^2-1|$ = 0.940) agrees with the centrosymmetric nature of römerite. The crystal structure of römerite was refined, using *Shelxl*-2014 (Sheldrick, 2015), starting from the atomic coordinates given by Fanfani *et al.* (1970). After several cycles of isotropic refinement, the R_1 factor converged to 0.082, thus indicating the correctness of the structural model. Two H atoms hosted at H4 and H13 showed high U_{eq} values and were thus removed; the correct position of both was then found in the difference-Fourier map. Moreover, taking into account the results of the electron microprobe analysis, the site scattering at the Fe1 site was modeled using the Fe *vs* Mg scattering curves taken from the *International Tables for Crystallography* (Wilson, 1992). After the introduction of anisotropic displacement parameters for cations (but H), the R_1 factor converged to 0.067, and lowered to 0.054 assuming the anisotropism of the O atoms of the SO_4 groups. In order to avoid too short O-H distances, a soft restraint on these distances was applied. An aniso-

Table 2 - Crystal data and summary of parameters describing data collection and refinement for römerite.

Crystal data	
Crystal size (mm)	0.12 × 0.09 × 0.07
Cell setting, space group	Triclinic, $P\bar{1}$
a (Å)	6.4512(6)
b (Å)	15.323(2)
c (Å)	6.3253(6)
α (°)	90.131(5)
β (°)	100.900(4)
γ (°)	85.966(4)
V (Å^3)	612.41(10)
Z	1
Data collection and refinement	
Radiation, wavelength (Å)	Mo$K\alpha$, λ = 0.71073
Temperature (K)	293
Maximum observed 2θ (°)	70.82
Measured reflections	14275
Unique reflections	4719
Reflections with $F_o > 4\sigma(F_o)$	4346
R_{int} after absorption correction	0.0168
$R\sigma$	0.0167
Range of h, k, l	$-10 \leq h \leq 10$ $-24 \leq k \leq 22$ $-10 \leq l \leq 9$
R_1 [F_o>4 σ F_o]	0.0234
R_1 (all data)	0.0262
wR_2 (on F_o^2)	0.0697
Goodness of fit	1.103
Number of least-squares parameters	226
Maximum and minum residual peak (e/Å^3)	0.61 (at 0.74 Å from O2) -0.56 (at 0.79 Å from S2)

tropic model for all the atom positions (except the H ones) converged to 0.0234 for 4346 reflections with $F_o > 4\sigma(F_o)$ and 226 refined parameters. Details of data collection and crystal structure refinement are reported in Table 2. Table 3 reports atomic coordinates, site occupancies, and isotropic or equivalent isotropic displacement parameters. Selected bond distances for cations are shown in Table 4.

DESCRIPTION OF THE CRYSTAL STRUCTURE

General features and cation coordinations

The general features of the crystal structure of römerite agree with those reported by Fanfani *et al.* (1970). Following Schindler *et al.* (2006), it can be described as formed by a structural unit having chemical composition $2\times[Fe^{3+}(SO_4)_2(H_2O)_4]^-$ and an interstitial complex of composition $\{Fe^{2+}(H_2O)_6\}^{2+}$, weakly bonded to each other through H-bonds (Fig. 3).

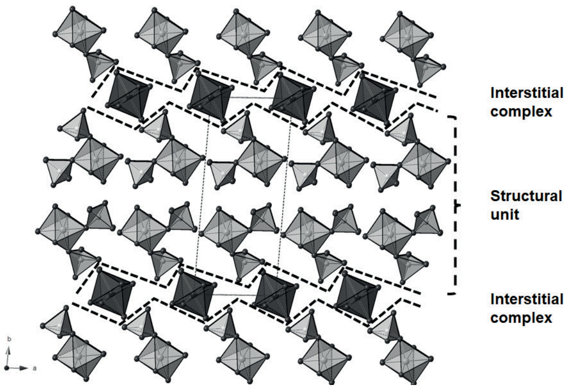

Fig. 3 - Projection along **c** of the crystal structure of römerite.

Ferrous iron is hosted at the Fe1 site and it is six-fold coordinated by H_2O groups. Bond distances range between 2.082 (Fe1-Ow3) and 2.125 Å (Fe1-Ow1), with an average <Fe-Ow> distance of 2.108 Å, agreeing with the average value reported by Fanfani *et al.* (1970), *i.e.* 2.112 Å. The refined site occupation factor (s.o.f.) points to a minor substitution of Fe^{2+} by Mg^{2+}, in agreement with the chemical data. On the basis of the refined s.o.f., the calculated BVS at the Fe1 site is 2.14 valence unit (v.u.) (Table 5).

Ferric iron, hosted at the Fe2 site, is octahedrally coordinated by four H_2O groups and two oxygen atoms; the latter belong to two different SO_4 groups, giving rise to a $[Fe^{3+}(SO_4)_2(H_2O)_4]^-$ cluster having a *cis*-configuration of ligands in the octahedron. The average distance at the Fe2 site is 1.998 Å; the average <Fe-O> distance (1.942 Å) is shorter than <Fe-Ow> (2.027 Å). The calculated BVS is 3.17 v.u. (Table 5).

Two independent SO_4 groups occur, both bonded to the Fe2-centered octahedron through corner-sharing. Average <S-O> distances are 1.471 and 1.469 Å for S1 and S2, respectively, in agreement with the average <S-O> distance in sulfates, *i.e.* 1.473 Å (Hawthorne *et al.*, 2000). The BVS values are 6.07 and 6.09 v.u. for S1 and S2, respectively. In agreement with Fanfani *et al.* (1970), the lengthening of S-O distances for oxygen atoms bonded to the Fe^{3+} ion is observed. Indeed, S1-O1 and S2-O5 are 1.496 and 1.494 Å, definitely longer than the other S-O bonds.

Hydrogen bonding

The interstitial complex $\{Fe^{2+}(H_2O)_6\}^{2+}$ and the structural unit $2\times[Fe^{3+}(SO_4)_2(H_2O)_4]^-$ are connected to each other by means of H-bonds. Indeed, the examination of the BVS at the fifteen independent anion positions (Table 5) shows that only O1 and O5 have values close to 2 v.u., whereas the other anions are underbonded. Some of them (O2, O3, O4, O6, O7, and O8) belong to SO_4 groups and have BVS ranging between 1.52

Table 3 - Atoms, site occupancy factors (s.o.f.), fractional atomic coordinates, and isotropic (*) or equivalent isotropic displacement parameters (in Å^2) for römerite.

Site	**s.o.f.**	***x/a***	***y/b***	***z/c***	$U_{eq/iso}$
Fe1	$Fe_{0.93(1)}Mg_{0.07(1)}$	0	0	0	0.0233(1)
Fe2	$Fe_{1.00}$	0.33834(3)	0.32049(2)	0.59415(3)	0.01584(5)
S1	$S_{1.00}$	0.59254(5)	0.16805(2)	0.36383(2)	0.01818(6)
S2	$S_{1.00}$	0.75975(4)	0.38681(2)	0.90753(5)	0.01631(6)
O1	$O_{1.00}$	0.4325(2)	0.20875(7)	0.4840(2)	0.0265(2)
O2	$O_{1.00}$	0.5827(2)	0.2182(1)	0.1649(2)	0.0373(3)
O3	$O_{1.00}$	0.8060(2)	0.17060(7)	0.4946(2)	0.0267(2)
O4	$O_{1.00}$	0.5391(2)	0.07822(8)	0.3233(2)	0.0393(3)
O5	$O_{1.00}$	0.6215(2)	0.33040(8)	0.7571(2)	0.0310(2)
O6	$O_{1.00}$	0.6434(2)	0.42237(7)	0.0678(2)	0.0289(2)
O7	$O_{1.00}$	0.8250(2)	0.45656(7)	0.7822(2)	0.0315(2)
O8	$O_{1.00}$	0.9446(2)	0.33050(7)	0.0082(2)	0.0256(2)
Ow1	$O_{1.00}$	0.2481(3)	0.0497(1)	0.8682(3)	0.0490(4)
Ow2	$O_{1.00}$	0.1125(2)	0.0492(1)	0.3104(2)	0.0406(3)
Ow3	$O_{1.00}$	0.1762(3)	0.8826(1)	0.0914(2)	0.0512(4)
Ow4	$O_{1.00}$	0.2577(2)	0.2556(8)	0.8433(2)	0.0253(2)
Ow5	$O_{1.00}$	0.0350(2)	0.30762(7)	0.4418(2)	0.0233(2)
Ow6	$O_{1.00}$	0.2183(2)	0.43552(7)	0.6971(2)	0.0276(2)
Ow7	$O_{1.00}$	0.3780(2)	0.38788(7)	0.3344(2)	0.0282(2)
H1	$H_{1.00}$	0.335(4)	0.009(2)	0.829(5)	0.070(9)*
H2	$H_{1.00}$	0.330(8)	0.079(3)	0.975(7)	0.17(2)*
H3	$H_{1.00}$	0.253(3)	0.057(2)	0.333(5)	0.08(1)*
H4	$H_{1.00}$	0.048(5)	0.081(2)	0.400(5)	0.08(1)*
H5	$H_{1.00}$	0.182(4)	0.863(2)	0.219(3)	0.049(7)*
H6	$H_{1.00}$	0.238(5)	0.847(2)	0.006(4)	0.064(9)*
H7	$H_{1.00}$	0.365(4)	0.240(2)	0.959(4)	0.056(8)*
H8	$H_{1.00}$	0.150(3)	0.279(2)	0.897(4)	0.047(7)*
H9	$H_{1.00}$	-0.035(4)	0.264(1)	0.478(4)	0.046(7)*
H10	$H_{1.00}$	0.005(4)	0.316(1)	0.298(3)	0.037(6)*
H11	$H_{1.00}$	0.274(5)	0.473(2)	0.809(4)	0.09(1)*
H12	$H_{1.00}$	0.082(3)	0.439(2)	0.730(5)	0.059(8)*
H13	$H_{1.00}$	0.313(5)	0.442(1)	0.290(5)	0.08(1)*
H14	$H_{1.00}$	0.476(4)	0.381(2)	0.248(4)	0.055(8)*

and 1.59 v.u., whereas atoms hosted at Ow1-Ow7 are severely undersaturated, with BVS from 0.34 to 0.51 v.u. This observation, coupled with the location of H atoms during the crystal structure refinement, highlights the important role played by H-bonds in römerite. Table 6 gives the details of H-bonds.

Oxygen atoms belonging to SO_4 groups and not coordinated to Fe^{3+} ions act as acceptors of H-bonds; calculating the corresponding bond strengths according to Ferraris & Ivaldi (1988), their corrected BVS range between 1.96 and 2.09 v.u.

With respect to the model proposed by Fanfani *et al.* (1970), the higher quality of the present crystal structure allowed a more accurate description of the H-bond system. Indeed, minor differences, related to bonds involving the H_2O groups hosted at Ow1 and Ow7, have been found. The Ow1 site shows the H-bond Ow1-H2···O4, in agreement with the unpublished results of Westland (2012). On the contrary, according to Fanfani *et al.* (1970), H2 does not seem to be involved in the H-bond system, although H2 could be involved in an Ow1···Ow4 bond, with a relatively

Table 4 - Selected bond distances (in Å) for römerite.

Fe1	– Ow3	2.082(1) ×2	S1	– O4	1.453(1)
	– Ow2	2.117(1) ×2		– O2	1.465(1)
	– Ow1	2.125(1) ×2		– O3	1.469(1)
				– O1	1.496(1)
	average	2.108		average	1.471
Fe2	– O5	1.936(1)	S2	– O6	1.455(1)
	– O1	1.948(1)		– O7	1.463(1)
	– Ow7	2.008(1)		– O8	1.464(1)
	– Ow6	2.031(1)		– O5	1.494(1)
	– Ow4	2.033(1)			
	– Ow5	2.034(1)			
	average	1.998		average	1.469

Table 5 - Weighted bond valence sums (in valence unit) for römerite.

Site	Fe1	Fe2	S1	S2	Σv_a	Σv_a(corr)
O1		$0.60^{\times 1\downarrow}$	$1.42^{\times 1\downarrow}$		2.02	2.02
O2			$1.54^{\times 1\downarrow}$		1.54	1.96
O3			$1.52^{\times 1\downarrow}$		1.52	2.09
O4			$1.59^{\times 1\downarrow}$		1.59	2.08
O5		$0.62^{\times 1\downarrow}$		$1.42^{\times 1\downarrow}$	2.04	2.04
O6				$1.58^{\times 1\downarrow}$	1.58	2.02
O7				$1.54^{\times 1\downarrow}$	1.54	2.01
O8				$1.54^{\times 1\downarrow}$	1.54	2.02
Ow1	$0.34^{\times 2\downarrow}$				0.34	0.03
Ow2	$0.35^{\times 2\downarrow}$				0.35	0.04
Ow3	$0.38^{\times 2\downarrow}$				0.38	-0.01
Ow4		$0.48^{\times 1\downarrow}$			0.48	-0.03
Ow5		$0.48^{\times 1\downarrow}$			0.48	0.04
Ow6		$0.48^{\times 1\downarrow}$			0.48	0.04
Ow7		$0.51^{\times 1\downarrow}$			0.51	0.04
Σv_c	2.14	3.17	6.07	6.09		

Note: right superscripts indicate the number of equivalent bonds involving anions.
For sites with mixed occupancy, BVS have been weighted according to the proposed site population. Σv_a(corr) = BVS corrected taking into account H-bonds.
Bond parameters after Brese & O'Keeffe (1991) were used.

Table 6 - Hydrogen-bond lengths (in Å) and angles (in °) for römerite.

Donor (D)	D–H	Acceptor (A)	H···A	D–H···A angle	D···A
Ow1–H1	0.872(17)	O4	1.877	163.8	2.726(2)
Ow1–H2	0.911(19)	O4	2.358	148.9	3.173(2)
Ow2–H3	0.906(18)	O4	1.909	169.2	2.804(2)
Ow2–H4	0.891(18)	O3	2.173	156.5	3.011(2)
Ow3–H5	0.856(16)	O3	1.870	174.9	2.724(2)
Ow3–H6	0.893(17)	O2	1.952	169.6.	2.835(2)
Ow4–H7	0.924(17)	O2	1.741	174.0	2.662(2)
Ow4–H8	0.887(16)	O8	1.750	177.1	2.636(2)
Ow5–H9	0.885(16)	O3	1.833	168.7	2.707(2)
Ow5–H10	0.900(15)	O8	1.812	178.9	2.712(2)
Ow6–H11	0.940(18)	O6	1.853	156.2	2.739(2)
Ow6–H12	0.938(17)	O7	1.755	173.9	2.689(2)
Ow7–H13	0.915(17)	O7	1.759	175.9	2.673(2)
Ow7–H14	0.912(17)	O6	1.855	152.7	2.698(2)

long distance of 3.17 Å (Fig. 4). This discrepancy is likely related to the lower quality of the crystal structure refinement performed using film data, although the relatively high U_{iso} value of H2 could suggest some kind of positional disorder.

According to Westland (2012), H14, bonded to Ow7, could be involved in a bifurcated H-bond with O2 and O6. Usually, bifurcated H-bonds are characterized by two relatively weak bonds, whereas in römerite the H-bond between Ow7 and O6 is relatively strong, showing an O···O distance of 2.698 Å and an Ow7-H14···O6 angle of 152.7°. On the contrary, the distance between Ow7 and O2 is definitely longer, *i.e.* 3.113 Å, with a very small angular value (115.2°) and a very long H···O distance (2.61 Å). In agreement with previous studies (*e.g.*, Brown, 1976; Anderson *et al.*, 2012), H···O distances longer than 2.5 Å and O-H···O angles smaller than 120° do not represent bonding interactions. Consequently, Ow7 likely forms an H-bond with O6 only. Taking into account the O···O distances and applying the relationship of Ferraris & Ivaldi (1988) between bond distance and bond strength, the corrected values of BVS at the Ow1-Ow7 sites range between -0.03 and 0.04 v.u., in agreement with their occupancy by H_2O groups.

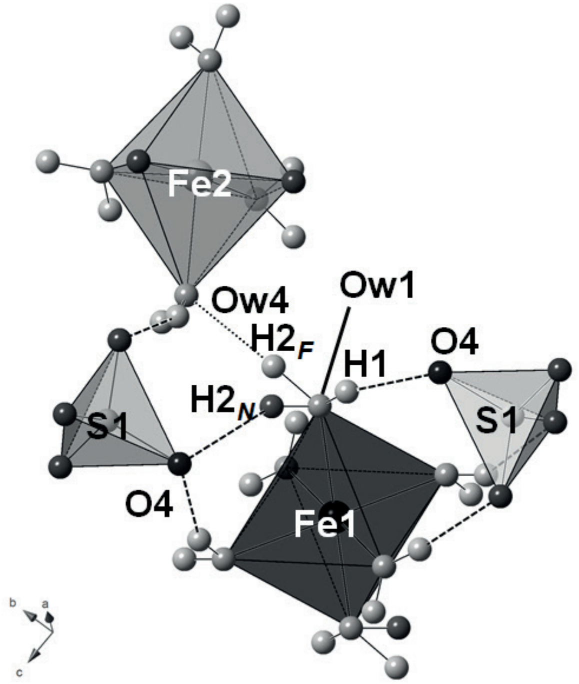

Fig. 4 - The different configurations of H-bond around Ow1 site. The labels of the atoms discussed in the text are shown. $H2_F$ and $H2_N$ indicate the position of the H atom in the structural model of Fanfani *et al.* (1970) and in the new model, respectively. Dashed lines represent H-bonds, whereas the dotted line represents the $H2_F\cdots$Ow4 contact in the model by Fanfani *et al.* (1970).

ACKNOWLEDGMENTS

This research received support by MIUR through the SIR 2014 project "THALMIGEN – Thallium: Mineralogy, Geochemistry, and Environmental Hazards" (Grant No. RBSI14A1CV), granted to CB. The University Centrum for Applied Geosciences (UGAC) is thanked for the access to the Eugen Friedrich Stumpfl electron microprobe laboratory. The authors are grateful to S. Merlino for his helpful advice. The constructive criticism of two anonymous reviewers improved the original manuscript.

REFERENCES

Anderson J.L., Peterson R.C., Swainson I., 2012. The atomic structure of deuterated boyleite $ZnSO_4\cdot4D_2O$, ilesite $MnSO_4\cdot4D_2O$, and bianchite, $ZnSO_4\cdot6D_2O$. *American Mineralogist* 97: 1905-1914.

Bandy M.C., 1938. Mineralogy of three sulphate deposits of northern Chile. *American Mineralogist* 23: 669-760.

Biagioni C., Bonaccorsi E., Orlandi P., 2011. Volaschioite, $Fe^{3+}_4(SO_4)O_2(OH)_6\cdot2H_2O$, a new mineral species from Fornovolasco, Apuan Alps, Tuscany, Italy. *The Canadian Mineralogist* 49: 605-614.

Brese N.E., O'Keeffe M., 1991. Bond-valence parameters for solids. *Acta Crystallographica* B47: 192-197.

Brown I.D., 1976. On the geometry of O-H···O hydrogen bonds. *Acta Crystallographica* A32: 24-31.

Bruker AXS Inc., 2004. Apex2. Bruker Advanced X-ray Solutions, Madison, Wisconsin, USA.

Chio C.H., Sharma S.K., Muenow D.W., 2005. Micro-Raman studies of hydrous ferrous sulfates and jarosites. *Spectrochimica Acta* A61: 2428-2433.

Fanfani L., Nunzi A., Zanazzi P.F., 1970. The crystal structure of roemerite. *American Mineralogist* 55: 78-89.

Ferraris G., Ivaldi G., 1988. Bond valence vs bond length in O···O hydrogen bonds. *Acta Crystallographica* B44: 341-344.

Frost R.L., Palmer S.J., Čejka J., Sejkora J., Plašil, J. Jebavá, I., Keeffe E.C., 2011. A Raman spectroscopic study of $M^{2+}M^{3+}$ sulphate minerals, römerite $Fe^{2+}Fe^{3+}{}_2(SO_4)_4\cdot14H_2O$ and botryogen $Mg^{2+}Fe^{3+}(SO_4)_2(OH)\cdot7H_2O$. *Journal of Raman spectroscopy* 42: 825-830.

Grailich J., 1858. Der Römerit, ein neues Mineral aus dem Rammelsberge, nebst Bemerkungen über die Bleiglätt. *Sitzungsberichte der Kaiserlichen Akademie der Wissenschaften* 28: 272-288.

Hawthorne F.C., Krivovichev S.V., Burns P.C., 2000. The crystal chemistry of sulfate minerals. *Reviews in Mineralogy and Geochemistry* 40: 1-101.

Jambor J.L., Nordstrom D.K., Alpers C.N., 2000. Metal-sulfate salts from sulfide mineral oxidation. *Reviews in Mineralogy and Geochemistry* 40: 303-350.

Lin W., Chen G., 1990. Lishizhenite – A new zinc sulphate mineral. *Acta Mineralogica Sinica* 10: 299-305.

Mauro D., Biagioni C., Pasero M., 2018. Crystal-chemistry of sulfates from Apuan Alps (Tuscany, Italy). I. Crystal structure and hydrogen bond system of melanterite, $Fe(H_2O)_6(SO_4)\cdot H_2O$. *Periodico di Mineralogia* 87: 89-96.

Oleinikov B.V., Shvartsev S.L., 1968. Contemporary sulfate formation in the zone of oxidation of pyrrhotite-chalcopyrite hydrothermal ores, northwestern Siberian Platform. *Geologiya i Geofizika* 6: 15-25 (in Russian).

Schindler M., Huminicki D.M.C., Hawthorne F.C., 2006. Sulfate minerals. I. Bond topology and chemical composition. *The Canadian Mineralogist* 44: 1403-1429.

Sheldrick G.M., 2015. Crystal structure refinement with SHELXL. *Acta Crystallographica* C71: 3-8.

Smith D.G.W., Nickel E.H., 2007. A system for codification for unnamed minerals: report of the Subcommittee for Unnamed Minerals of the IMA Commission on New Minerals, Nomenclature and Classification. *The Canadian Mineralogist* 45: 983-1055.

Van Loan P.R., Nuffield E.W., 1959. An X-ray study of römerite. *The Canadian Mineralogist* 6: 348-356.

Westland R.E., 2012. New phases in the hydrous ferric sulfate system, a supporting argument that the mineral lausenite is of formula $Fe_2(SO_4)_3\cdot5H_2O$ and the crystal structure refinement and hydrogen bonding scheme of the minerals quenstedtite and romerite. Unpublished thesis, Queen's University, Kingston, Ontario, Canada: 161 p.

Wilson A.J.C. (editor), 1992. International Tables for Crystallography Volume C: Mathematical, Physical and Chemical Tables. Kluwer Academic Publishers, Dordrecht, The Netherlands.

Wolfe C.W., 1937. Re-orientation of roemerite. *American Mineralogist* 22: 736-741.

(ms. pres. 19 aprile 2018; ult. bozze 25 giugno 2018)

Edizioni ETS
Palazzo Roncioni - Lungarno Mediceo, 16, I-56127 Pisa
info@edizioniets.com - www.edizioniets.com
Finito di stampare nel mese di febbraio 2019